Linköping studies in Science and Technology. Dissertations No. 320

Utdrag ur:

Linogram and Other Direct Fourier Methods for Tomographic Reconstruction

Maria Magnusson
Department of Electrical Engineering
Linköping University, S-581 83 Linköping, Sweden
Linköping 1993

1.1 MRI

The images produced by MRI (Magnetic Resonance Imaging) are similar to those produced by CT in the sense that they represent cross-sections of the human body. MRI is described in for example [Mac83], [Kak87], [Edh93a], and [Weh91]. Here, we will give a simplified description of MRI in terms of classical physics as well as a simplified description of two reconstruction methods.

MRI is based on the fact that any atom with an odd number of nucleons (protons or neutrons) has a magnetic moment, which is due to the *spin* of the nucleus. When the atom is placed in a strong magnetic field, the magnetic moment of the nucleus tends to line up with the field. The magnetic moment can then be perturbed by another rotating magnetic field. This causes the magnetic moment to *precess*. After the perturbation, during the return to equilibrium state a radio frequency signal is emitted. This signal can be measured and reconstruction methods can be applied to compute an image of the precessing nuclei density distribution inside the object.

The totally dominating measured element is the hydrogen nucleus, consisting of one single proton. Hydrogen is abundant in the human body, in water, fat, and all organic substances. Thus simplistically, MRI normally measures the hydrogen density in the human body.

The magnetic moment is associated with an angular momentum. The magnetic moment $\overline{m}$ [Am^2] and the angular momentum $\overline{L}$ [Nms] are related as

$$\overline{m} = \gamma \overline{L}, \tag{1.1}$$

where γ [Am/Ns] is the gyro-magnetic ratio, a property of the material. When the magnetic moment is placed in a strong magnetic field $\overline{B_0}$ it tends to line up with the field. In classical physics (see for example [Duf80]), it is well-known that a static magnetic field $\overline{B_0}$ acts on an angular momentum with a torque. The torque influences the angular momentum (and therefore also the magnetic moment) to precess like a gyroscope around the direction of the static magnetic field, see Fig. 1.1 .

It can be shown [Duf80] that the precessing frequency, called the *Larmor frequency,* is

$$\omega_0 = \gamma B_0, \tag{1.2}$$

where ω_0 [rad/s] is the angular frequency, γ [Am/Ns] is the gyro-magnetic ratio, and B_0 [N/Am]=[Vs/m^2] is the static magnetic field.

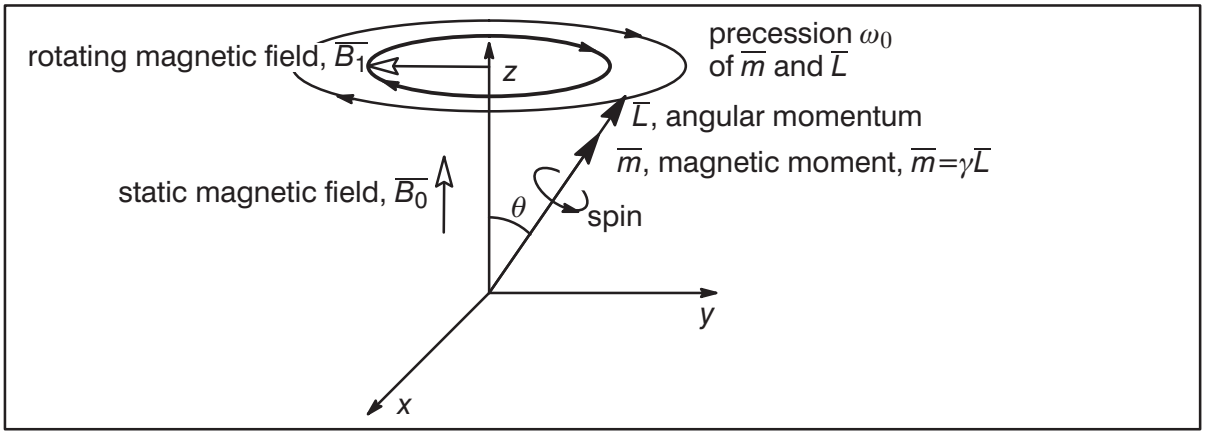

Fig. 1.1 The magnetic moment $\overline{m}$ precesses in the static magnetic field $\overline{B_0}$.

In reality the topic is more complicated than we have indicated here. Among other things, we know from quantum mechanics that the angular momentum of any system can only take certain discrete values. Here we have not taken the discreteness under consideration. Fortunately, the classical theory will give the same result as the quantum mechanic approach if small partial volume elements consisting of several nuclei are regarded instead of individual nuclei.

The hydrogen nuclei can be *excited* by a rotating magnetic field generated by coils around the object. The frequency of this rotating field must be equal to the Larmor frequency ω_0 to obtain **resonance**, otherwise the excitation will be negligible. In our classical model the excitation causes the precession angle θ to increase according to

$$\theta = \gamma B_1 t_p, \tag{1.3}$$

where t_p is the duration of the rotating magnetic field pulse $\overline{B_1}$, see Fig. 1.1 . Common values of $\overline{B_0}$ are 0.1−2 T. This gives resonance frequencies ω_0 in the radio frequency range of 3−60 MHz. The excitation signal is often called ”the radio frequency signal” because of this frequency range.

If the static strong magnetic field ($\overline{B_0}$) lies in the z-direction and the rotating magnetic field ($\overline{B_1}$) lies in the xy-plane, as in Fig. 1.1 , the total vector field $\overline{B}$ is given by

$$\overline{B} = \overline{B_0} + \overline{B_1} = B_0\hat{z} + B_1(\hat{x}\cos\omega_0 t + \hat{y}\sin\omega_0 t) \tag{1.4}$$

where $\hat{x}, \hat{y}$, and $\hat{z}$ are unit vectors.

After the time t_p the excitation field $\overline{B_1}$ is turned off. The precession of the nuclei then undergoes FID (free induction decay) as they return to their equilibrium state. During this process an electromagnetic signal at the Larmor frequency $\omega_0=\gamma B_0$ is emitted. This signal

can be detected by the same coils that earlier produced the rotating magnetic field. The signal is proportional to the hydrogen nuclei density of the material.

A hydrogen nucleus returns to its equilibrium state with the time constant T_1 known as the longitudinal or spin-lattice relaxation time. The transverse or spin-spin relaxation time, T_2 determines the time for the individual magnetic moments to come out of phase. There are also a third, more practical parameter T_2^* which includes T_2 as well as local inhomogeneities of the static magnetic field. Because of physical constraints the following relationship always holds

$$T_2^* \leq T_2 \leq T_1. \tag{1.5}$$

The various time constants and the process of first exciting the nuclei and then letting them return to their equilibrium state are illustrated in Fig. 1.2 . Note that the coordinate system rotates with the Larmor frequency around the z-axis.

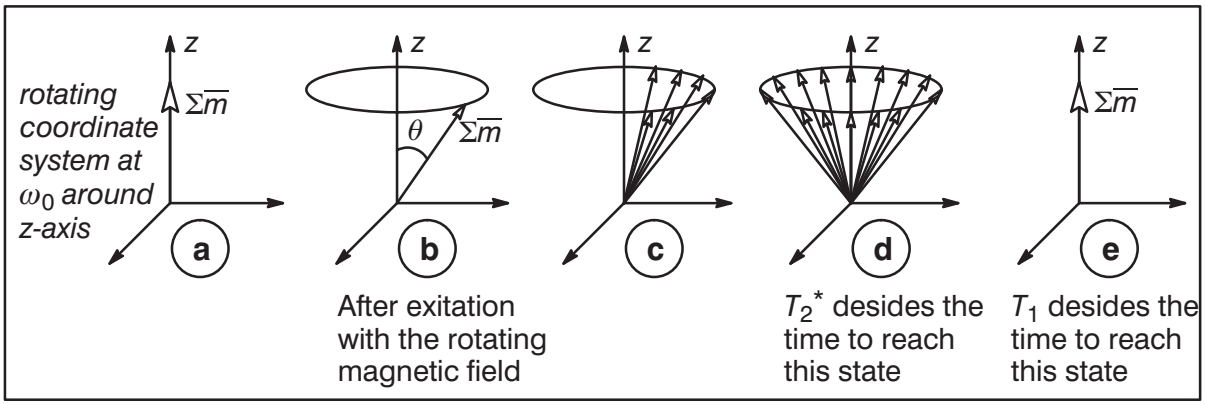

Fig. 1.2 The process of first exiting the nuclei and then letting them return to their equilibrium state.

- **a)** The sum of the nuclei magnetic moments $\Sigma\overline{m}$ lines up with the static magnetic field $\overline{B_0}$.
- **b)** A radio frequency rotating magnetic field pulse at frequency ω_0 and a certain duration is applied which causes the magnetic moments to precess around the z-axis an angle θ and frequency ω_0.
- **c)** The magnetic moments have started to return to equilibrium state. Some of them have become out of phase.
- **d)** The time constant T_2^* determines the time when all magnetic moments are out of phase.
- **e)** The time constant T_1 determines the time when all magnetic moments have returned to equilibrium state.

The FID signal is attenuated both according to the T_1 and T_2^* time constants. Some typical values for T_1 and T_2^* are 0.5s and 50 ms, respectively. Except for imaging the nuclei density, imaging of the time constants T_1 and T_2^* can provide useful images since the relation T_1/T_2^* differs greatly between various tissues of the human body. For the sake of brevity, however, we restrict our discussion to reconstruction of images of the nuclei density.

We are going to give a simplified description of two of the more common methods. The first reconstruction method is called **2D phase encoding**. To restrict the resonance and hence the excitation of hydrogen nuclei to a single z-plane, a linear magnetic field gradient

$$\Delta B_z = G_z z \tag{1.6}$$

is applied in the z-direction and superimposed on $\overline{B_0}$, see Fig. 1.3 a. Therefore, when a rotating magnetic field at the Larmor frequency $\omega_0=\gamma B_0$ is applied, only hydrogen nuclei near plane $z=0$ will be excited. After a while, when the spin vectors have obtained a desired precessing angle θ (usually 90°), the excitation signal and the z-gradient is turned off as shown in Fig. 1.4 . The nuclei in plane $z=0$ are now precessing with the frequency ω_0.

Next, a gradient in the y-direction

$$\Delta B_y = G_y y \tag{1.7}$$

is applied as shown in Fig. 1.3 b. The gradient pulse will last for a certain time T as shown in Fig. 1.4 . The nuclei along different y-coordinates will then start to precess at different Larmor frequencies and change their phases according to

$$\phi_y = \omega t = \gamma(B_0 + \Delta B_y)T = \gamma(B_0 + G_y y)T = \omega_0 T + \gamma G_y y T = \omega_0 T + k_y y \tag{1.8}$$

where

$$k_y = \gamma G_y T \tag{1.9}$$

and ω_0 is the Larmor frequency associated with B_0. After the y-gradient is turned off, the nuclei at different y-coordinates are precessing with different phase angles at the frequency ω_0.

Then, a gradient in the x-direction

$$\Delta B_x = G_x x \tag{1.10}$$

is applied as shown in Fig. 1.3 c and the response FID-signal in the measuring coil is measured, see Fig. 1.4 . The nuclei along different x-coordinates are now precessing at different Larmor frequencies

$$\omega_x = \gamma(B_0 + \Delta B_x) = \gamma(B_0 + G_x x) = \omega_0 + \gamma G_x x = \omega_0 + \frac{k_x}{t} x \tag{1.11}$$

where

$$k_x = \gamma G_x t \tag{1.12}$$

giving

$$\phi_x = \omega_x \cdot t = \omega_0 t + k_x x. \tag{1.13}$$

The nuclei density $f(x,y)$ at each point (x,y) now precesses at phase

$$\phi = \phi_x + \phi_y. \tag{1.14}$$

and amplitud

$$f(x,y). \tag{1.15}$$

Equation (1.14) and (1.15) can be combined to the following signal

$$f(x,y) \cdot \exp[-j\phi] = f(x,y) \cdot e^{-j\phi}. \tag{1.16}$$

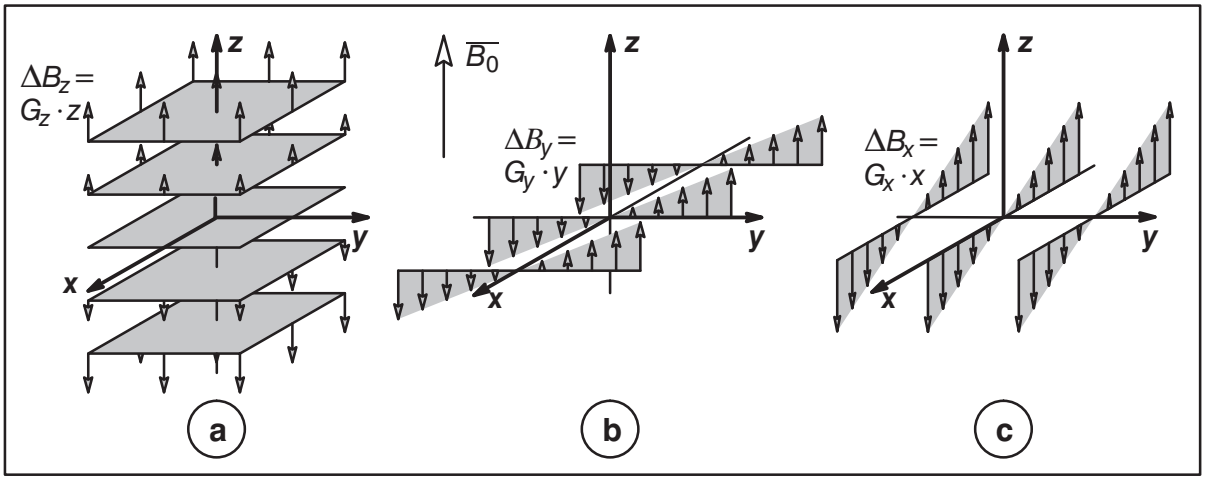

Fig. 1.3 Magnetic gradients applied during an MRI examination

a) The gradient $\Delta B_z = G_z \cdot z$ during the application of the excitation magnetic field.

b) The gradient $\Delta B_y = G_y \cdot y$ during the phase encoding.

c) The gradient $\Delta B_x = G_x \cdot x$ during the FID measure.

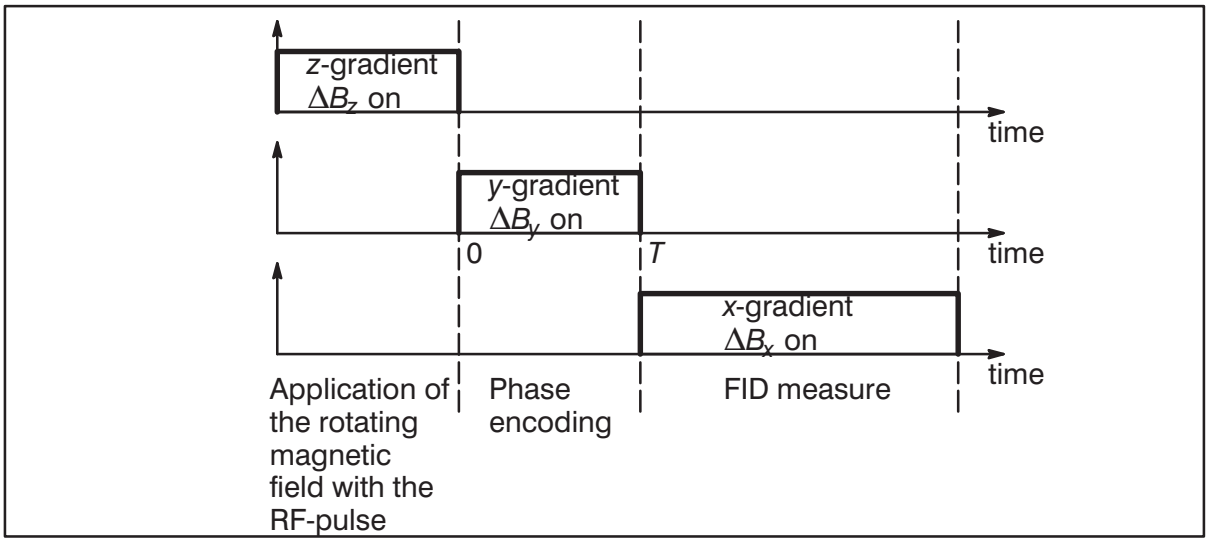

Fig. 1.4 A time diagram for the application of magnetic field gradients. Readout of *one* row in the Fourier domain of nuclei density.

The total measured signal is then

$$s(t) = \int\int f(x,y) \cdot \exp[-jyk_y] \cdot \exp[-jxk_x(t)] \cdot \exp[-j\omega_0 t]\, dxdy =$$

$$= \boldsymbol{F}(k_x(t), k_y)\big|_{k_y = const} \cdot \exp[-j\omega_0 t]. \tag{1.17}$$

where we have used (1.16), (1.14), (1.13) and (1.8). Since $\omega_0 T$ in (1.8) is a constant, it is not necessary to include it in (1.17). The (k_x,k_y) is the spatial frequency domain, usually called the k-space, see Fig. 1.5 . In order to acquire data for the whole k-space, we need to step the phase-coding gradient k_y through a sequence of different values and repeat the readout several times as shown in Fig. 1.6 .

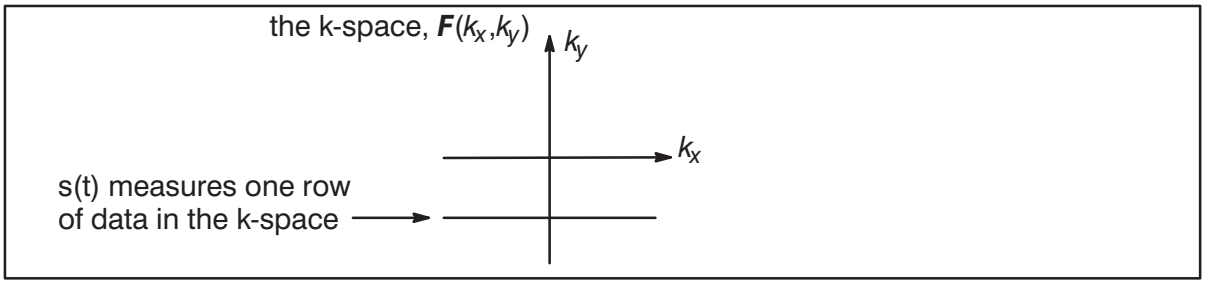

Fig. 1.5 The measured signal s(t) measures one row in the 2D Fourier domain $\boldsymbol{F}(k_x,k_y)$ of the nuclei density $f(x,y)$.

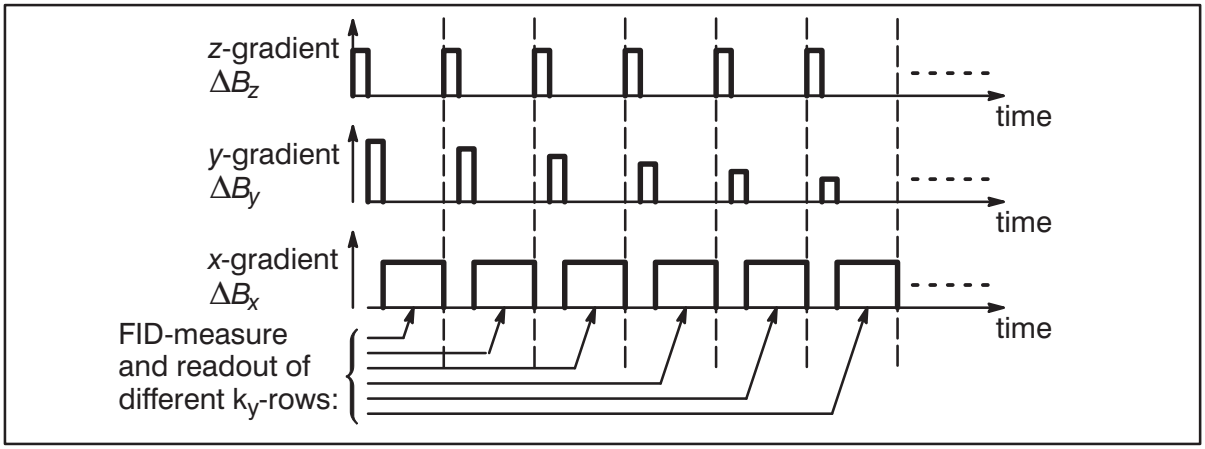

Fig. 1.6 A time diagram for the application of magnetic field gradients. Readout of *several* rows k_y in the Fourier domain of nuclei density.

The totally measured 2D signal is then

$$\int\int f(x,y)\ \exp[-jyk_y]\ \exp[-jxk_x]\ \exp[-j\omega_0 t]\,dxdy\ =\ \boldsymbol{F}(k_x,k_y)\ \exp\big[-j\omega_0 t\big]. \qquad (1.18)$$

It is not difficult to see that after multiplication with $\exp[j\omega_0 t]$ on both sides of (1.18), the remaining part $\boldsymbol{F}(k_x,k_y)$ is the 2D Fourier transform of $f(x,y)$, the target function. i.e.

$$\boldsymbol{F}(k_x,k_y)\ =\ \int\int f(x,y)\ \cdot\ \exp[-jyk_y]\ \cdot\ \exp[-jxk_x]\,dxdy. \qquad (1.19)$$

From (1.19), $f(x,y)$ is easily obtained by inverse 2D FFT.

Since this reconstruction method implies only Fourier transforms it is very fast. However, other types of nuclei than hydrogen may have time constants T_1 and T_2^* which are too short for the phase-encoding method to work. Then other, more slowly, methods must be used.

MRI is presently undergoing a very lively development. 2D-images as well as whole 3D-volumes with higher resolution and more sample points are produced. Other nuclei than the hydrogen are of great interest for the clinicians and are beginning to be exploited. Not only the anatomy, but also the dynamic physiology of the human body can be visualized by fast 3D-imaging. Various new contrast fluids used together with MRI give images with new information.

In Fig. 1.7 , an MRI-image and a CT-image is shown to the left and right, respectively. The CT-image is a horizontal slice of the human head, which is the only practically viable orientation for CT cross-sections. The MRI-technique is more flexible with regard to orientation and to produce the vertical slice in Fig. 1.7 a is no problem whatsoever. MRI- and CT-images show different things. MRI shows (mainly) hydrogen nucleus density, while CT shows matter density. Bone matter, for example, gives a large signal in CT. In Fig. 1.7 b, the white material is the skull. In MRI, on the other hand, bone gives no signal. Consequently, the skull forms a black area between the grey skin and the grey brain in Fig. 1.7 a.

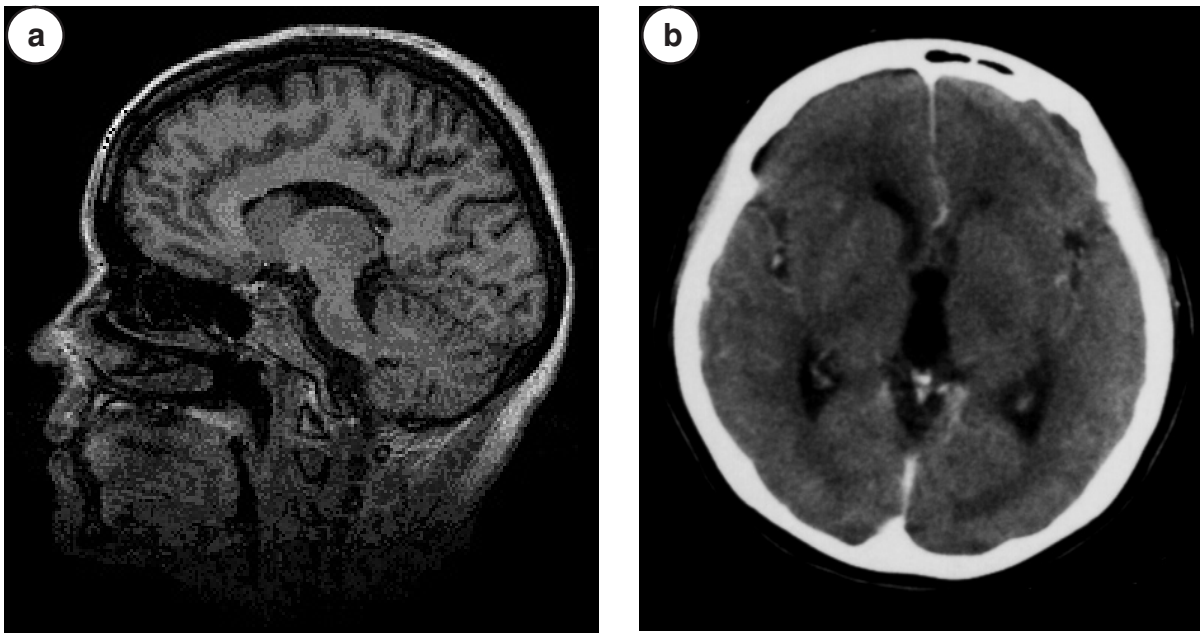

Fig. 1.7 Cross-sectional images of the human head, different techniques. **a)** MRI. **b)** CT.